

**Octupole degree of freedom for the critical-point candidate
nucleus ^{152}Sm in a reflection-asymmetric relativistic mean-field
approach**

W. Zhang,^{1,2} Z. P. Li,¹ S. Q. Zhang ^{*,1} and J. Meng ^{†3,1,4}

¹*State Key Laboratory of Nuclear Physics and Technology,*

School of Physics, Peking University,

Beijing 100871, People's Republic of China

²*School of Electrical Engineering and Automation,*

He'nan Polytechnic University, Jiaozuo 454003, People's Republic of China

³*School of Physics and Nuclear Energy Engineering,*

Beihang University, Beijing 100191, People's Republic of China

⁴*Department of Physics, University of Stellenbosch, Stellenbosch, South Africa*

(Dated: November 6, 2018)

Abstract

The potential energy surfaces of even-even $^{146-156}\text{Sm}$ are investigated in the constrained reflection-asymmetric relativistic mean-field approach with parameter set PK1. It is shown that the critical-point candidate nucleus ^{152}Sm marks the shape/phase transition not only from $U(5)$ to $SU(3)$ symmetry, but also from the octupole-deformed ground state in ^{150}Sm to the quadrupole-deformed ground state in ^{154}Sm . By including the octupole degree of freedom, an energy gap near the Fermi surface for single-particle levels in ^{152}Sm with $\beta_2 = 0.14 \sim 0.26$ is found, and the important role of the octupole deformation driving pair $\nu 2f_{7/2}$ and $\nu 1i_{13/2}$ is demonstrated.

PACS numbers: 21.10.-k, 21.60.Jz, 27.70.+q

* Email: sqzhang@pku.edu.cn

† Email: mengj@pku.edu.cn

I. INTRODUCTION

The first-order phase transition between spherical $U(5)$ and axially deformed $SU(3)$ shapes [1, 2] has received widespread attention in the past decade. It was shown that ^{152}Sm and other $N = 90$ isotones are the empirical examples of the analytic description of nuclei at the critical point of such a transition [3]. Theoretical studies on the phase transition were typically based on phenomenological geometric models of nuclear shapes and potentials [2] and algebraic models of nuclear structure [4]. The first calculations, establishing a link between dynamical symmetry models and microscopic theories, were carried out using the relativistic mean-field (RMF) approximation in the Sm isotopes [5]. Along this line, much work was done using either relativistic [6–9] or nonrelativistic approaches [10–12].

Normally the regions of nuclei with strong octupole correlations correspond to either the proton or neutron numbers close to 34 ($1g_{9/2} \leftrightarrow 2p_{3/2}$ coupling), 56 ($1h_{11/2} \leftrightarrow 2d_{5/2}$ coupling), 88 ($1i_{13/2} \leftrightarrow 2f_{7/2}$ coupling), and 134 ($1j_{15/2} \leftrightarrow 2g_{9/2}$ coupling) [13]. A variety of approaches were applied to investigate the role of the octupole degree of freedom in Sm and the neighboring nuclear region. The Woods-Saxon-Bogoliubov cranking model is used to study the shapes of rotating Xe, Ba, Ce, Nd, and Sm nuclei with $N = 84 - 94$ and the expectations of octupole-deformed mean fields at low and medium spins are confirmed [14]. The *spdf* interacting boson model is applied to Sm isotopes with $N = 86 - 92$ to examine the signatures of octupole correlations [15]. Based on a collective rotation-vibration Hamiltonian in which the axial quadrupole and octupole degrees of freedom are coupled, the energy levels and electromagnetic transition probabilities for $N = 90$ isotones are well reproduced [16].

Very recently, a new $K^\pi = 0^-$ octupole excitation band was observed in ^{152}Sm and a pattern of repeating excitations built on the 0_2^+ level similar to those built on the ground state emerges [17]. It was suggested that ^{152}Sm , rather than a critical-point nucleus, is a complex example of shape coexistence [17].

Based on the investigations mentioned previously, it is timely and necessary to investigate the Sm isotopes in a microscopic and self-consistent approach with the octupole degree of freedom. The newly developed reflection-asymmetric relativistic mean-field (RAS-RMF) approach is a good candidate for this purpose [18] considering the remarkable success of RMF theory [19–21] in describing many nuclear phenomena related to stable nuclei [19], exotic nuclei [22, 23], as well as supernova and neutron stars [24]. In Ref. [18], the RAS-

RMF approach was first applied to the well-known octupole-deformed nucleus ^{226}Ra , and reproduced well both the binding energy and deformation.

In this article, the RAS-RMF approach will be applied to investigate the potential energy surfaces (PES) of even-even $^{146-156}\text{Sm}$ isotopes in the (β_2, β_3) plane and the shape evolution involving the octupole degrees of freedom will be analyzed.

II. FORMALISM

The basic ansatz of the RMF theory is a Lagrangian density where nucleons are described as Dirac particles that interact via the exchange of various mesons and the photon. The mesons considered are the isoscalar-scalar σ , the isoscalar-vector ω , and the isovector-vector ρ . The effective Lagrangian density reads [25]

$$\begin{aligned} \mathcal{L} = & \bar{\psi} \left[i\gamma^\mu \partial_\mu - M - g_\sigma \sigma - g_\omega \gamma^\mu \omega_\mu - g_\rho \gamma^\mu \vec{\tau} \cdot \vec{\rho}_\mu - e\gamma^\mu \frac{1 - \tau_3}{2} A_\mu \right] \psi \\ & + \frac{1}{2} \partial^\mu \sigma \partial_\mu \sigma - \frac{1}{2} m_\sigma^2 \sigma^2 - \frac{1}{3} g_2 \sigma^3 - \frac{1}{4} g_3 \sigma^4 \\ & - \frac{1}{4} \Omega^{\mu\nu} \Omega_{\mu\nu} + \frac{1}{2} m_\omega^2 \omega^\mu \omega_\mu + \frac{1}{4} c_3 (\omega^\mu \omega_\mu)^2 \\ & - \frac{1}{4} \vec{R}^{\mu\nu} \cdot \vec{R}_{\mu\nu} + \frac{1}{2} m_\rho^2 \vec{\rho}^\mu \cdot \vec{\rho}_\mu \\ & - \frac{1}{4} F^{\mu\nu} F_{\mu\nu}, \end{aligned} \quad (1)$$

in which the field tensors for the vector mesons and the photon are, respectively, defined as

$$\begin{cases} \Omega_{\mu\nu} = \partial_\mu \omega_\nu - \partial_\nu \omega_\mu, \\ \vec{R}_{\mu\nu} = \partial_\mu \vec{\rho}_\nu - \partial_\nu \vec{\rho}_\mu, \\ F_{\mu\nu} = \partial_\mu A_\nu - \partial_\nu A_\mu. \end{cases} \quad (2)$$

Using the classical variational principle, one can obtain the Dirac equation for the nucleons and the Klein-Gordon equations for the mesons. To solve these equations, we employ the basis expansion method, which was widely used in both the nonrelativistic and relativistic mean-field models. For axial-symmetric reflection-asymmetric systems, where nonaxial quadrupole and octupole deformations are plainly excluded, the spinors are expanded in

terms of the eigenfunctions of the two-center harmonic-oscillator (TCHO) potential

$$V(r_{\perp}, z) = \frac{1}{2}M\omega_{\perp}^2 r_{\perp}^2 + \begin{cases} \frac{1}{2}M\omega_1^2(z + z_1)^2, & z < 0 \\ \frac{1}{2}M\omega_2^2(z - z_2)^2, & z \geq 0 \end{cases} \quad (3)$$

where M is the nucleon mass, z_1 and z_2 (real, positive) represent the distances between the centers of the spheroids and their intersection planes, and $\omega_1(\omega_2)$ are the corresponding oscillator frequencies for $z < 0$ ($z \geq 0$) [18]. The TCHO basis was widely used in studies of fission, fusion, heavy-ion emission, and various cluster phenomena [26]. By setting proper asymmetric parameters, the major and the z -axis quantum numbers are real numbers very close to integers, and the integers are used in the Nilsson-like notation $\Omega[Nn_z m_l]$ for convenience. More details can be found in Ref. [18].

The binding energy at a certain deformation is obtained by constraining the mass quadrupole moment $\langle \hat{Q}_2 \rangle$ to a given value μ_2 [27]

$$\langle H' \rangle = \langle H \rangle + \frac{1}{2}C(\langle \hat{Q}_2 \rangle - \mu_2)^2 \quad (4)$$

where C is the curvature constant parameter and μ_2 is the given quadrupole moment. The expectation value of \hat{Q}_2 is $\langle \hat{Q}_2 \rangle = \langle \hat{Q}_2 \rangle_n + \langle \hat{Q}_2 \rangle_p$ with $\langle \hat{Q}_2 \rangle_{n,p} = \langle 2r^2 P_2(\cos \theta) \rangle_{n,p}$. The deformation parameter β_2 is related to $\langle \hat{Q}_2 \rangle$ by $\langle \hat{Q}_2 \rangle = \frac{3}{\sqrt{5\pi}} Ar^2 \beta_2$ with $r = R_0 A^{1/3}$ ($R_0 = 1.2$ fm) and A the mass number. The octupole moment constraint can also be applied similarly with $\langle \hat{Q}_3 \rangle = \langle \hat{Q}_3 \rangle_n + \langle \hat{Q}_3 \rangle_p$, $\langle \hat{Q}_3 \rangle_{n,p} = \langle 2r^3 P_3(\cos \theta) \rangle_{n,p}$, and $\langle \hat{Q}_3 \rangle = \frac{3}{\sqrt{7\pi}} Ar^3 \beta_3$. By constraining the quadrupole moment and octupole moment simultaneously, the total energy surface in the (β_2, β_3) plane can be obtained.

III. RESULTS AND DISCUSSION

The properties of even-even $^{146-156}\text{Sm}$ are calculated in the constrained RAS-RMF approach with parameter set PK1 [28]. The parameter set PK1 is one of the best parameter sets available in the framework of RMF theory, which, as usual, is obtained by fitting the masses of selected spherical nuclei as well as saturation properties of nuclear matter. The success of universal RMF parameter sets was demonstrated for describing the properties of spherical [19] and deformed nuclei [20, 21], and they are believed to be appropriate for application in octupole-deformed nuclei. In return, the application for octupole-deformed nuclei

TABLE I: The total binding energy (in MeV) as well as the quadrupole deformation β_2 and octupole deformation β_3 of the ground states of even-even $^{146-156}\text{Sm}$ obtained in the constrained RAS-RMF approach with PK1, in comparison with the available experimental data.

Nucleus	E^{cal}	β_2^{cal}	β_3^{cal}	E^{exp} [29]	β_2^{exp} [30]
^{146}Sm	1213.38	0.09	0.07	1210.91	—
^{148}Sm	1227.27	0.14	0.08	1225.39	0.14
^{150}Sm	1241.59	0.18	0.13	1239.25	0.19
^{152}Sm	1254.46	0.20	0.15	1253.10	0.31
^{154}Sm	1267.76	0.32	0.00	1266.94	0.34
^{156}Sm	1280.08	0.33	0.02	1279.99	—

will also provide a further test. The TCHO basis with 16 major shells for both fermions and bosons is used. The pairing correlations are treated by the BCS approximation with a constant pairing gap $\Delta = 11.2/\sqrt{A}$ MeV.

The binding energy, quadrupole, and octupole deformations are listed for the ground states of $^{146-156}\text{Sm}$ in Table I. The binding energies are well reproduced within 0.2%. Moreover, excellent agreement is obtained for the quadrupole deformations except ^{152}Sm (see the discussion in the following).

To investigate the shape evolution in the Sm isotopes, the contour plots of the total energies as functions of β_2 and β_3 for $^{146-156}\text{Sm}$ are shown in Fig. 1, which have up-down symmetry in the (β_2, β_3) plane because of the equivalence between the states with positive and negative β_3 .

It is shown in Fig. 1 that for the ground states, $^{146,148}\text{Sm}$ are near spherical, ^{150}Sm octupole deformed, and $^{154,156}\text{Sm}$ well deformed while ^{152}Sm marks the transition from octupole to quadrupole deformed. In detail, for ^{146}Sm , with $N = 84$ close to the magic number 82, the ground state is near spherical with $(\beta_2, \beta_3)=(0.08, 0.08)$. For ^{148}Sm and ^{150}Sm , with increasing neutron number, the deformations (β_2, β_3) gradually increase. Particularly for ^{150}Sm with $N = 88$, a global minimum with substantial quadrupole and octupole deformations $(\beta_2, \beta_3)=(0.19, 0.14)$ is well developed, which is about 1.36 MeV deeper than the corresponding quadrupole-deformed state. For ^{152}Sm , the global minimum moves to

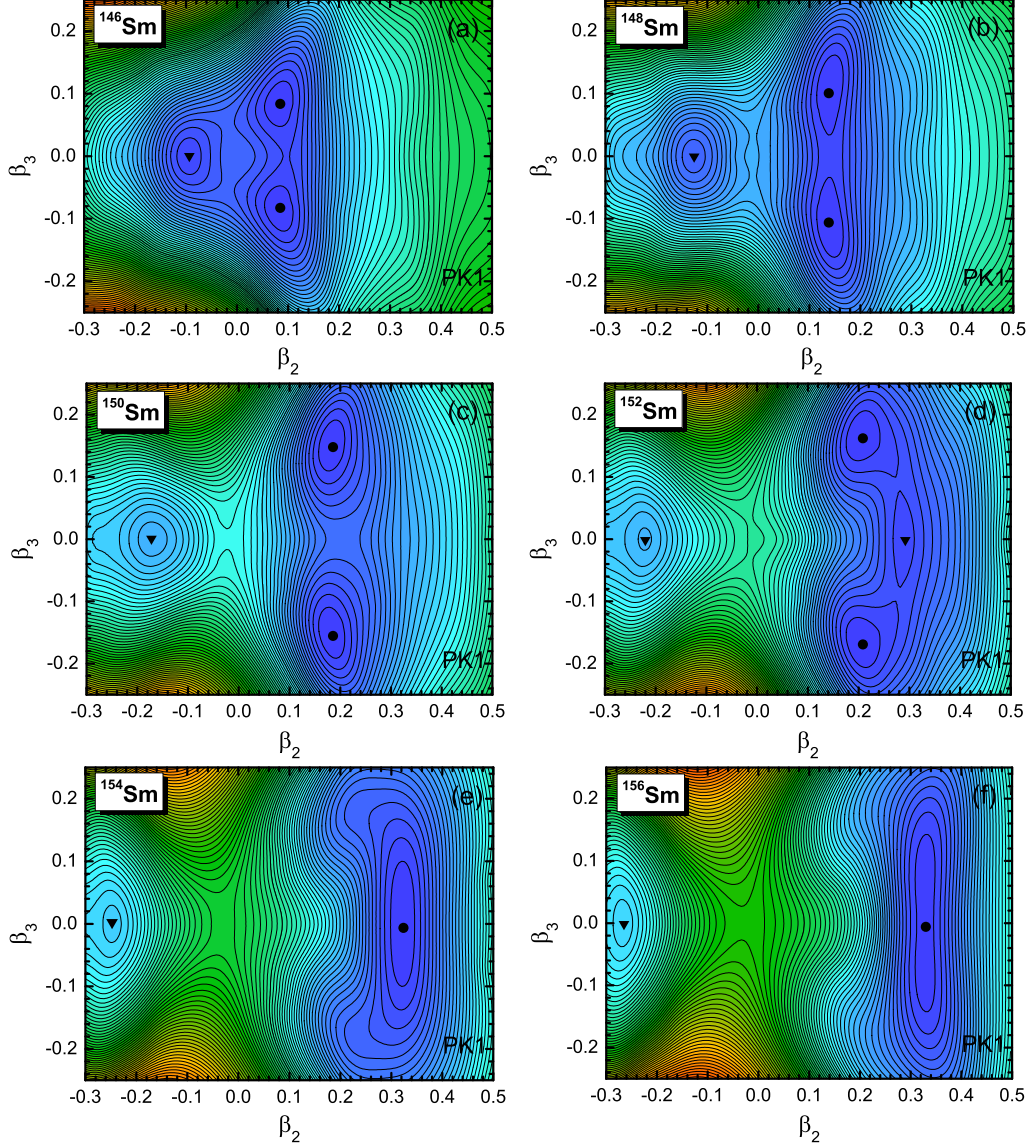


FIG. 1: (Color online) The contour plots of total energies for the even-even $^{146-156}\text{Sm}$ in (β_2, β_3) plane obtained in the RAS-RMF approach with PK1 and constant- Δ pairing. The energy separation between contour lines is 0.25 MeV. The global minima and other local minima are denoted by “•” and “▼”, respectively.

$(\beta_2, \beta_3)=(0.20, 0.15)$, while a quadrupole minimum emerges at $(\beta_2, \beta_3)=(0.29, 0)$. It is interesting to note that the deformation of this minimum is quite close to the experimental value $\beta_2^{\text{exp}} = 0.31$ [30] listed in Table I. The energy difference between the two minima is 0.33 MeV with a 0.5 MeV barrier in between. For $^{154,156}\text{Sm}$, the ground states are well quadrupole deformed with $(\beta_2, \beta_3) \sim (0.33, 0)$. Similar PES's can also be obtained with

other parameter sets such as NL3 [31]. In addition, one notes that the oblate minima shown in Fig. 1 may not be stable against the γ direction [9].

In Ref. [5], axially deformed RMF calculation with a variety of effective interactions was performed for $^{144-158}\text{Sm}$ to discuss the transition from spherical $U(5)$ to axially deformed $SU(3)$ shapes. It was shown that the PES's of $^{144,146}\text{Sm}$ are minimized near spherical and of $^{154-158}\text{Sm}$ well-deformed, while in between the PES's of $^{148,150,152}\text{Sm}$ are found to be relatively flat. From Fig. 1, it is shown that the conclusion remains to be true even with the inclusion of the octupole degree of freedom.

Meanwhile, we do find something new for ^{152}Sm after including the octupole degree of freedom, that is, ^{152}Sm marks the shape/phase transition not only from $U(5)$ to $SU(3)$ symmetry, but also from the octupole-deformed to quadrupole-deformed case.

Quite recently in Ref. [17], a new $K^\pi = 0^-$ band was observed, which has a remarkable similarity in its $E1$ transition to the first excited $K^\pi = 0^+$ band as the lowest $K^\pi = 0^-$ band to the ground-state band. A pattern of repeating excitations built on the 0_2^+ level similar to those built on the ground state is claimed to indicate that ^{152}Sm is a complex example of shape coexistence rather than a critical-point nucleus. These observations can be well understood from the PES obtained previously. For ^{152}Sm with the octupole minimum at $(\beta_2, \beta_3)=(0.20, 0.15)$ and the quadrupole minimum at $(\beta_2, \beta_3)=(0.29, 0)$, if one performs the generator coordinate method (GCM) [27, 32] calculation with the PES, two low-lying states in the (β_2, β_3) plane with similar quadrupole deformation will be obtained, which are a mixture of quadrupole and octupole deformation configurations. Based on these two states, the pattern of repeating excitations is expected.

To understand the evolution of the octupole deformation microscopically, the neutron single-particle levels in ^{152}Sm for the states minimized with respect to β_3 and the states with $\beta_3 = 0$ for $\beta_2 = 0.14 \sim 0.26$ are shown in Fig. 2. The levels near the Fermi surface are labeled by Nilsson-like notations $\Omega[Nn_z m_l]$ of the largest component. In the left panel of Fig. 2, a large energy gap with $N = 88$ near the Fermi surface is found, which is related to the softness of the potential energy surface in the quadrupole and octupole degrees of freedom in ^{152}Sm . There is no obvious neutron gap near the Fermi surface for the states with $\beta_3 = 0$. In addition, the proton single-particle levels for the corresponding states are shown in Fig. 3, where no obvious energy gaps can be found near the Fermi surfaces.

It is well known that for nuclei with $N \sim 88$ or $Z \sim 56$ the octupole deformation

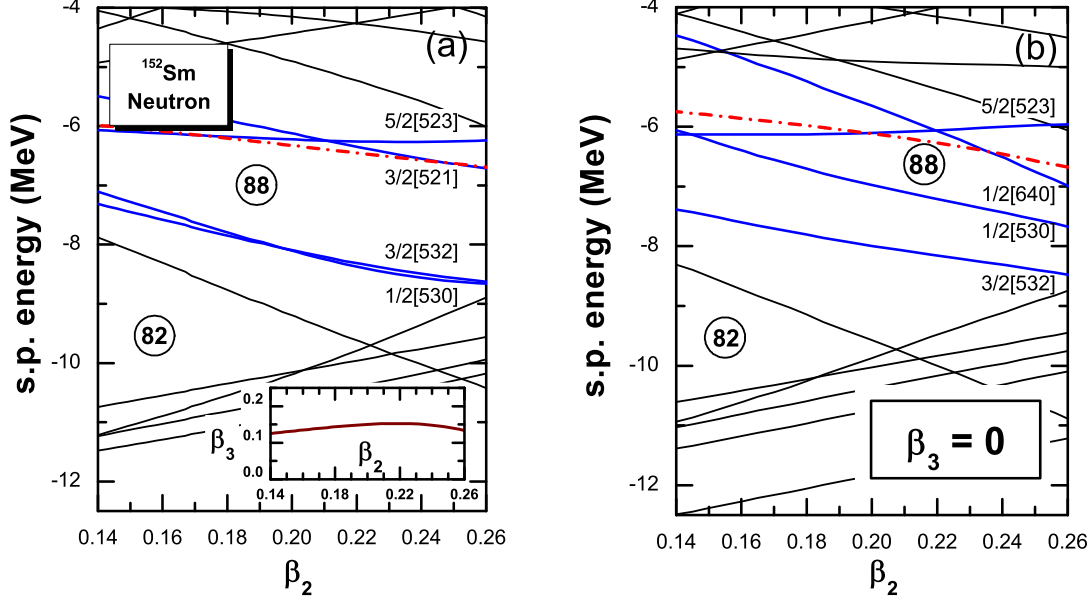


FIG. 2: (Color online) Neutron single-particle levels of ^{152}Sm in RAS-RMF approach with PK1 as functions of β_2 for states minimized with respect to β_3 (left panel) and states with $\beta_3 = 0$ (right panel). The dash-dot lines denote the corresponding Fermi surfaces. The levels near the Fermi surface are labeled by Nilsson-like notations $\Omega[Nn_z m_l]$ of the first component at $\beta_2 = 0.20$. The corresponding β_3 are shown in the inset.

driving pairs of orbitals include $(\nu 2f_{7/2}, \nu 1i_{13/2})$ and $(\pi 2d_{5/2}, \pi 1h_{11/2})$, which in the axially deformed case will be subgrouped as $(\nu 1/2[541], \nu 1/2[660])$, $(\nu 3/2[532], \nu 3/2[651])$, $(\nu 5/2[523], \nu 5/2[642])$, $(\nu 7/2[514], \nu 7/2[633])$, and $(\pi 1/2[431], \pi 1/2[550])$, $(\pi 3/2[422], \pi 3/2[541])$, $(\pi 5/2[413], \pi 5/2[532])$, respectively. It is interesting to investigate the performance of such pairs in the single-particle levels near the Fermi surfaces in Figs. 2 and 3. These levels together with their BCS occupation probabilities and corresponding contributions from the four leading components are shown in Table II. Taking the level $\nu 3/2[521]$ as an example, its second (20.1%) and third (15.5%) components compose an octupole deformation driving pair $(\nu 3/2[532], \nu 3/2[651])$. Similarly, one can find the pair $(5/2[523], 5/2[642])$ for $\nu 5/2[523]$, the pair $(3/2[532], 3/2[651])$ for $\nu 3/2[532]$, and the pair $(1/2[541], 1/2[660])$ (the fifth component $1/2[660]$ with 6.0%, which is not listed in Table II) for $\nu 1/2[530]$. However, for the proton side, no octupole deformation driving pairs are found among the four leading components. Therefore the neutron orbital takes a more important role in the evolution of octupole deformation in Sm isotopes than the proton one, consistent with the

energy gaps presented in Fig. 2.

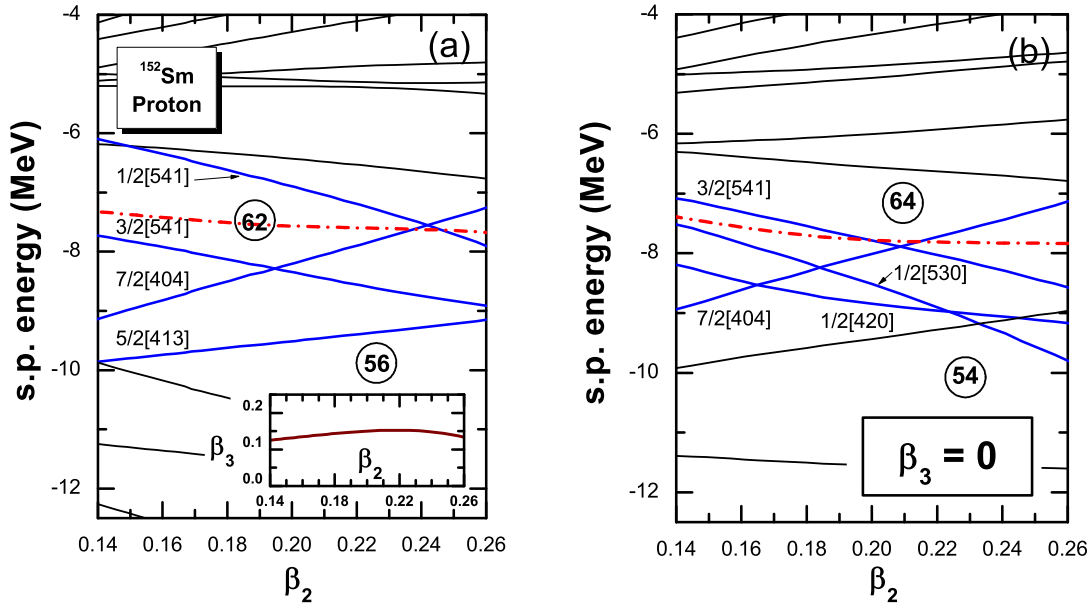


FIG. 3: (Color online) Same as Fig. 2, but for proton.

IV. CONCLUSION

In this article, the PES's of even-even $^{146-156}\text{Sm}$ in the (β_2, β_3) plane are obtained by the constrained RAS-RMF approach, and the single-particle levels near the Fermi surfaces for the nucleus ^{152}Sm are studied. It is shown that the critical-point candidate nucleus ^{152}Sm marks the shape/phase transition not only from $U(5)$ to $SU(3)$ symmetry, but also from the octupole-deformed ground state in ^{150}Sm to quadrupole-deformed ground state in ^{154}Sm .

Furthermore, the microscopic PES for the nucleus ^{152}Sm is consistent with the claimed shape coexistence based on the observation of repeating excitations built on the 0^+ level similar to those built on the ground state [17].

By including the octupole degree of freedom, an energy gap near the Fermi surface for single-particle levels in ^{152}Sm with $N = 88$ and $\beta_2 = 0.14 \sim 0.26$ is found, which is related to the softness of its potential energy surface in the quadrupole and octupole degrees of freedom. From the energy gap and the components of the single-particle levels near the Fermi surface, it is demonstrated that the neutrons play an important role for the octupole deformation driving in ^{152}Sm .

TABLE II: Single-particle levels near the Fermi surface for the ground state with $(\beta_2, \beta_3) = (0.20, 015)$ in ^{152}Sm together with their BCS occupation probabilities and corresponding contributions from the four leading components. The components originating from the octupole deformation driving pairs of orbitals $(\nu 2f_{7/2}, \nu 1i_{13/2})$ and $(\pi 2d_{5/2}, \pi 1h_{11/2})$ are in bold.

level	occu.	1st comp.		2nd comp.		3rd comp.		4th comp.	
$\nu 3/2[521]$	0.401	$3/2[521]$	33.3%	$3/2[532]$	20.1%	$3/2[651]$	15.5%	$3/2[631]$	9.4%
$\nu 5/2[523]$	0.434	$5/2[523]$	57.2%	$5/2[532]$	16.0%	$5/2[642]$	6.7%	$5/2[633]$	5.2%
$\nu 3/2[532]$	0.946	$3/2[532]$	46.4%	$3/2[541]$	21.1%	$3/2[512]$	8.8%	$3/2[651]$	5.8%
$\nu 1/2[530]$	0.947	$1/2[530]$	33.9%	$1/2[541]$	18.1%	$1/2[510]$	8.0%	$1/2[651]$	6.2%
$\pi 1/2[541]$	0.219	$1/2[420]$	21.4%	$1/2[541]$	21.4%	$1/2[440]$	17.7%	$1/2[521]$	9.8%
$\pi 7/2[404]$	0.763	$7/2[404]$	85.9%	$7/2[413]$	7.3%	$7/2[514]$	2.8%	$7/2[604]$	0.4%
$\pi 3/2[541]$	0.834	$3/2[541]$	34.6%	$3/2[411]$	20.0%	$3/2[521]$	17.9%	$3/2[532]$	9.1%
$\pi 5/2[413]$	0.952	$5/2[413]$	76.0%	$5/2[422]$	11.2%	$5/2[523]$	4.7%	$5/2[303]$	2.0%

ACKNOWLEDGMENTS

This work was supported, in part, by the Major State Basic Research Developing Program 2007CB815000, National Natural Science Foundation of China under Grant Nos 10775004, 10975007, and 10975008, China Postdoctoral Science Foundation, the Natural Science Foundation of He'nan Educational Committee under Grant No. 200614003, and the Young Backbone Teacher Support Program of He'nan Polytechnic University.

-
- [1] F. Iachello, N. V. Zamfir, and R. F. Casten, Phys. Rev. Lett. **81**, 1191 (1998).
 - [2] F. Iachello, Phys. Rev. Lett. **87**, 052502 (2001).
 - [3] R. F. Casten and N. V. Zamfir, Phys. Rev. Lett. **87**, 052503 (2001).
 - [4] P. Cejnar and J. Jolie, Prog. Part. Nucl. Phys. **62**, 210 (2009).
 - [5] J. Meng, W. Zhang, S. G. Zhou, H. Toki, and L. S. Geng, Eur. Phys. J. A **25**, 23 (2005).
 - [6] Z. Q. Sheng and J. Y. Guo, Mod. Phys. Lett. A **20**, 2711 (2005).
 - [7] R. Fossion, D. Bonatsos, and G. A. Lalazissis, Phys. Rev. C **73**, 044310 (2006).

- [8] T. Nikšić, D. Vretenar, G. A. Lalazissis, and P. Ring, Phys. Rev. Lett. **99**, 092502 (2007).
- [9] Z. P. Li, T. Nikšić, D. Vretenar, J. Meng, G. A. Lalazissis, and P. Ring, Phys. Rev. C **79**, 054301 (2009)
- [10] R. R. Rodríguez-Guzmán and P. Sarriguren, Phys. Rev. C **76**, 064303 (2007).
- [11] T. R. Rodríguez and J. L. Egido, Phys. Lett. **B663**, 49 (2008).
- [12] L. M. Robledo, R. R. Rodríguez-Guzmán, and P. Sarriguren, Phys. Rev. C **78**, 034314 (2008).
- [13] P. A. Butler and W. Nazarewicz, Rev. Mod. Phys. **68**, 349 (1996).
- [14] W. Nazarewicz and S. L. Tabor, Phys. Rev. C **45**, 2226 (1992).
- [15] M. Babilon, N. V. Zamfir, D. Kusnezov, E. A. McCutchan, and A. Zilges, Phys. Rev. C **72**, 064302 (2005).
- [16] N. Minkov, P. Yotov, S. Drenska, W. Scheid, D. Bonatsos, D. Lenis, and D. Petrellis, Phys. Rev. C **73**, 044315 (2006).
- [17] P. E. Garrett, W. D. Kulp, J. L. Wood *et al.*, Phys. Rev. Lett. **103**, 062501 (2009).
- [18] L. S. Geng, J. Meng, and H. Toki, Chin. Phys. Lett. **24**, 1865 (2007).
- [19] P. Ring, Prog. Part. Nucl. Phys. **37**, 193 (1996).
- [20] D. Vretenar, A. V. Afanasiev, G. A. Lalazissis, and P. Ring, Phys. Rep. **409**, 101 (2005).
- [21] J. Meng, H. Toki, S. G. Zhou, S. Q. Zhang, W. H. Long, and L. S. Geng, Prog. Part. Nucl. Phys. **57**, 470 (2006).
- [22] J. Meng and P. Ring, Phys. Rev. Lett. **77**, 3963 (1996).
- [23] J. Meng and P. Ring, Phys. Rev. Lett. **80**, 460 (1998).
- [24] N. K. Glendenning, *Compact Stars: Nuclear Physics, Particle Physics, and General Relativity* (Springer-Verlag, New York, 2000).
- [25] B. D. Serot and J. D. Walecka, Adv. Nucl. Phys. **16**, 1 (1986).
- [26] W. Greiner, J. Y. Park, and W. Scheid, *Nuclear Molecules* (World Scientific, Singapore, 1995).
- [27] P. Ring and P. Schuck, *The Nuclear Many-body Problem* (Springer-Verlag, New York, 1980).
- [28] W. H. Long, J. Meng, N. Van Giai, and S. G. Zhou, Phys. Rev. C **69**, 034319 (2004).
- [29] G. Audi, A. H. Wapstra, and C. Thibault, Nucl. Phys. **A729**, 337 (2003).
- [30] S. Raman, C. W. Nestor Jr., and P. Tikkanen, At. Data Nucl. Data Tables **78**, 1 (2001).
- [31] G. A. Lalazissis, J. König, and P. Ring, Phys. Rev. C **55**, 540 (1997).
- [32] J. M. Yao, J. Meng, P. Ring, and D. Vretenar, arXiv:0912.2650v1 [nucl-th].